DOR:

Research Paper

Experimental and Numerical Analysis of Local Lateral Compression Process of Metal Tubes between Cylindrical Shaped Dies

Hamzeh Kazemi[1], Heshmatollah Haghighat[2*]
[1]M.Sc. Graduate, Mechanical Engineering Department, Razi University, Kermanshah, Iran
[2]Associate Professor, Mechanical Engineering Department, Razi University, Kermanshah, Iran
[*]Email of Corresponding Authors: hhaghighat@razi.ac.ir
Received: November 13, 2023, Accepted: January 11, 2024

Abstract
Metal tubes are widely used in various forms in engineering structures. Local deformation of the tube is required due to design considerations or the tube's location in the machine or structure to facilitate its installation. This paper investigates the process of locally laterally compressing aluminum tubes using experimental and numerical simulation methods. The tube is positioned horizontally on the fixed lower die and is subjected to compressive load by the upper die, which is connected to the movable ram of the press machine, resulting in plastic deformation. Both upper and lower dies are semi-cylindrical with equal radii, and their axes are perpendicular to the tube's axis. For the experimental and numerical analysis, two types of aluminum 6061-T6 tubes with the same outer diameter but different inner diameters were chosen, and three similar samples were created for each type. The true stress behavior, based on the true strain of the aluminum material, was determined from a simple tensile test. Subsequently, the geometric dimensions of the deformed area of the tubes were measured for various press strokes. The geometric shape of the deformation zone and the experimental forming load data were compared with the simulation results obtained using ABAQUS software. A comparison between the results from the two experimental and simulation methods demonstrated good agreement.

Keywords
Tube Lateral Compression, Compression Force, Deformation Zone

1. Introduction

Metal tubes are widely used in the industry and are used in different geometric shapes in the construction of structures. They are also used for the transmission of fluids and gases in the construction of power transmission shafts, drills, and energy absorbers. To change the tubes into the desired shape, they are subjected to various forming processes. One of the forming processes is the local deformation of the tube. The local deformation of the tube is due to the design requirement or according to the position of the tube in the machine or structure, it is necessary to provide the possibility of installing the tube in its place. In this process, as in other metal forming processes, it is important to know the amount of necessary forming force and also the geometry of the tube after deformation. Several studies have been done in the field of tube forming.

Kobayashi and Daimarwa [1] conducted a series of experiments to investigate the deformation of ceramic tubes under lateral loading. They observed that in dynamic loading, the applied load and tube deflection at the moment of failure are greater than the values obtained in static loading. Avaleh and Gug Lo [2] proposed an experimental method based on image analysis to measure the strain field in tubes subjected to lateral deformation. They studied the tube as an energy absorber through practical experiments and theoretical methods. They measured the deformation field in the tube subjected to lateral plastic deformation using an optical technique. They found that the results were remarkably consistent with those previously obtained with strain gauges. Gupta et al. [3] paid attention to tubes as energy absorbers. As a result of the applied load, the tubes undergo plastic deformation in several different states, and each state has a related energy loss capacity. They conducted experimental and numerical investigations on mild steel aluminum tubes with different diameter-to-thickness ratios under quasi-static lateral loading. The deformation of the tubes was also investigated and analyzed with the help of the finite element method and the experimental and calculated results were compared. Niknejad et al. [4] experimentally investigated the effect of polyurethane filling foam on lateral plastic deformation in brass tubes under radial quasi-static loading. For this purpose, samples with five different diameters and thicknesses were prepared and for each fixed diameter of the samples, several tubes with different lengths were cut and all the samples participated in lateral pressure tests in empty and filled with polyurethane foam. According to the importance of accuracy of material properties as input data in finite element analysis due to their effect on output data, Rathnavira et al. [5] presented an improved method for determining the material properties of a tube based on the lateral compression process. For this purpose, they prepared three aluminum tubes with diameters of 32, 40, and 50 mm and subjected them to lateral pressure at a constant speed and vertical displacement of 20, 25, and 30 mm, and recorded the information about the compressive force and displacement, and finally, they were able to Mechanical properties such as yield strength and elastic modulus were obtained from the experimental data and the obtained results were compared with the reported results from uniaxial tensile tests. They showed that the proposed method can be used for easy and accurate prediction of tube material properties based on lateral plane strain compression test. Shiman et al. [6] used experimental analysis and numerical simulation methods to study the deformation of metal tubes during the forging process. Their goal was to investigate the depth of the folds in the inner part of the tube. The result was that the quality and structure of the tube surface had a great effect on the depth of the fold. In their investigation, the direction of force applied to the axis of the tube was the same. Nomura et al. [7] analyzed experimentally and numerically the process of local compression of aluminum rods between cylindrical and flat dies. The analyses were performed for different angles between the axis of the die and the axis of the rod. They concluded that the closer the angle of the die and the rod is to 45 degrees, the asymmetrical flow increases and the displacement of the two ends of the rod increases. They also concluded that performing the process with a 90-degree angle between the axis of the die and the rod causes tensile stress in the lower part of the rod, and this tensile stress is reduced by reducing the angle between the axis of the die and the rod. Parvizi Bina and Haghighat [8] predicted the billet cross-section geometry and calculated the necessary forming force in the process of plane strain lateral compression between flat dies and billets with a round cross-section. To analyze the process, they used two types of theoretical approaches, i.e. upper bound technique and the force balance analysis method. Also, they simulated the deformation process in DEFORM

software and concluded that the billet cross-section geometries predicted by analytical methods are in good agreement with the numerical simulation data. Pepelnjak et al. [9] obtained input data for numerical simulations of tube forming using the tube upsetting process. The flow curve of the analyzed tube was determined with a tube-shaped specimen. Guan et al. [10] proposed a novel process combining the flaring and upsetting deformation for forming the end flanges on thin-walled tubes. Zhang [11] studied the cross-sectional deformation of circular thin-walled tubes under lateral compression between two rigid plates in terms of the compressive force applied to the tube in the large elastic-plastic deformation stage during the lateral compressive process by both theoretical as well as finite element analysis methods.

In the mentioned studies, the tubes were under axial compression loading, or the entire length of the tube was subjected to lateral compression loading. In this paper, the plastic deformation of the tube in a part of its length under lateral compression loading is investigated. In the local compression process, the tube is placed horizontally between two cylindrical-shaped dies, and the tube is deformed by applying the external load. The process of local compression of the tube is investigated experimentally and also numerically using the ABAQUS software, and the results of the forming force and the geometry of the deformation area given by both methods, are compared for different process conditions.

2. Experimental tests

2.1 Making dies and tubes

In the process of local compression, the tube is placed horizontally between two similar cylindrical shaped dies, upper and lower dies, and by applying compressive force, the tube deforms plastically. As shown in Figure 1, the axis of the tube is perpendicular to the longitudinal axis of the die. To conduct the test, the tube was made of 6061-T6 aluminum alloy. Aluminum is a light metal that is abundant in nature. Pure aluminum does not have high strength which is why other elements such as copper, zinc, magnesium, and silicon are used to produce aluminum alloy to increase its strength. To make the tube, first, an aluminum rod was prepared and by turning it, two tubes with the same external diameter of 25 mm and different internal diameters were made. Figure 2 shows the cross-sectional dimensions of the tubes.

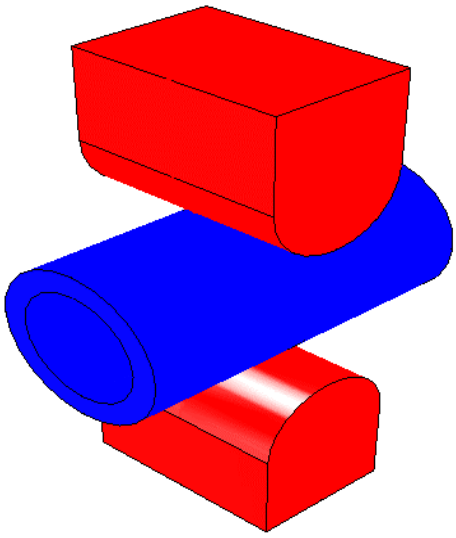

Figure 1. Positioning of the upper and lower cylindrical-shaped dies and the tube

The length of all samples is equal to 50 mm and three similar samples were made from both types of tubes. In Figure 3, two samples of manufactured tubes are shown.

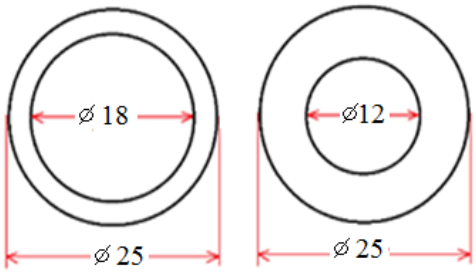

(a) (b)

Figure 2. Dimensions of the cross-sections of the samples

Figure 3. Two samples of tubes

A cylindrical rod with a diameter of 20 mm and made of CK45 steel is used as a die, i.e. the horizontal cylinder shown in Figure 4. The die tail, the vertical cylinder shown in Figure 4, was also made of CK45 steel with a diameter of 50 mm. A hole with a diameter of 20 mm is made to connect the die

set to the press jaw. The cylindrical die and its tail are welded together. Figure 4 shows the die placed on the tail. The top and bottom die sets are similar to each other.

Figure 4. Dies (horizontal cylinders) and die tails (vertical cylinders)

2.2 Simple tensile test

To determine the stress curve in terms of material strain, it is necessary to perform a simple tensile test. Since the studied metal is aluminum, a part of this standard known as ASTM-B557 is used. After determining the dimensions, according to the standard, the sample used in the simple tensile test is made. Figure 5 shows the fabricated sample.

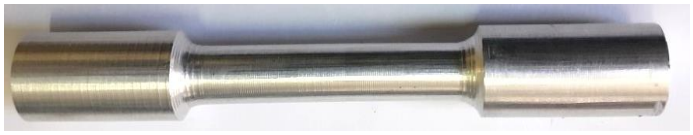

Figure 5. Sample prepared for simple tensile test

The information obtained from the simple tensile test is given in the form of the actual stress-strain curve in Figure 6.

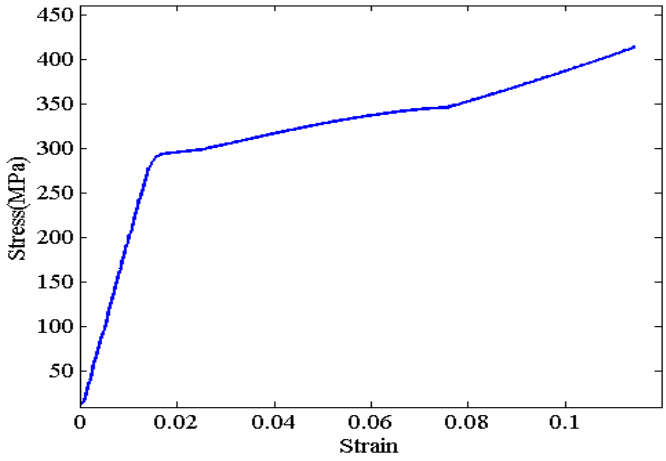

Figure 6. True stress-strain curve of aluminum material

2.3 Experimental tests

The position of placing the dies in the upper and lower jaws of the press machine and how to place the tube between the dies is shown in Figure 7.

Figure 7. The position of placing the tube between the dies in the press machine

To perform the test, first, the upper and lower dies are connected to the fixed and movable jaws of the press machine and each tube is placed horizontally on the lower die so that the middle of the length of the tube is in contact with the die. Then the pressure force is applied to the press machine. The forming process was repeated for different press strokes of 3, 6, and 9 mm and the curve of the changes in the forming force according to the press stroke was recorded by the machine. Blue and red colors are used to distinguish between the two groups of tubes. Each group of tubes was rolled on a cloth containing dye. The part of the tube that gets painted is not deformed and the part of the tube surface that remains unpainted is deformed. Figure 8 shows two groups of tubes for three different press strokes. According to the Figure, in the case of equal press strokes, as expected, a larger area of 18 mm inner diameter tubes (blue tubes) has been deformed.

Figure 8. Deformation areas in tubes with an inner diameter of 18 mm, blue color, and tubes with an inner diameter of 12 mm, red color

The graph of changes in compression force for a 3 mm press stroke in a tube with an inner diameter of 18 mm is shown in Figure 9. Due to the laxity of the system, the forming force was zero at first

and then started its upward trend. The amount of slack is 0.03 mm, and the maximum compressive forming force is 14.6 kN.

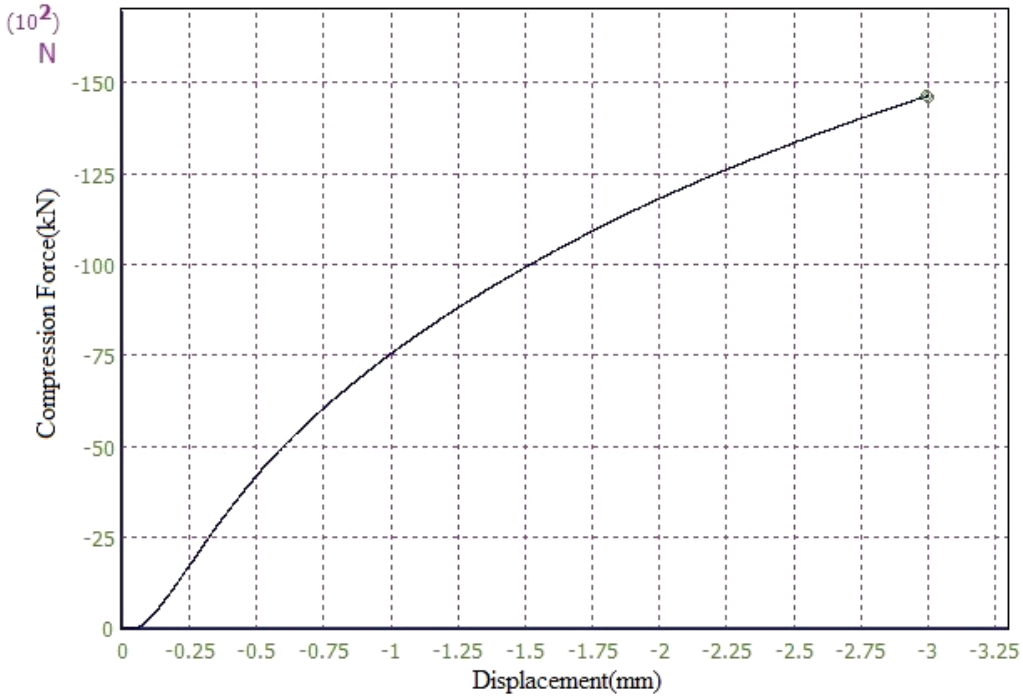

Figure 9. Compression force diagram for a 3 mm press stroke in a tube with an internal diameter of 18 mm

The graph of changes in compressive force for a 3 mm press stroke in a tube with an inner diameter of 12 mm is shown in Figure 10. According to the diagram shown, the maximum force is equal to 19.85 kN.

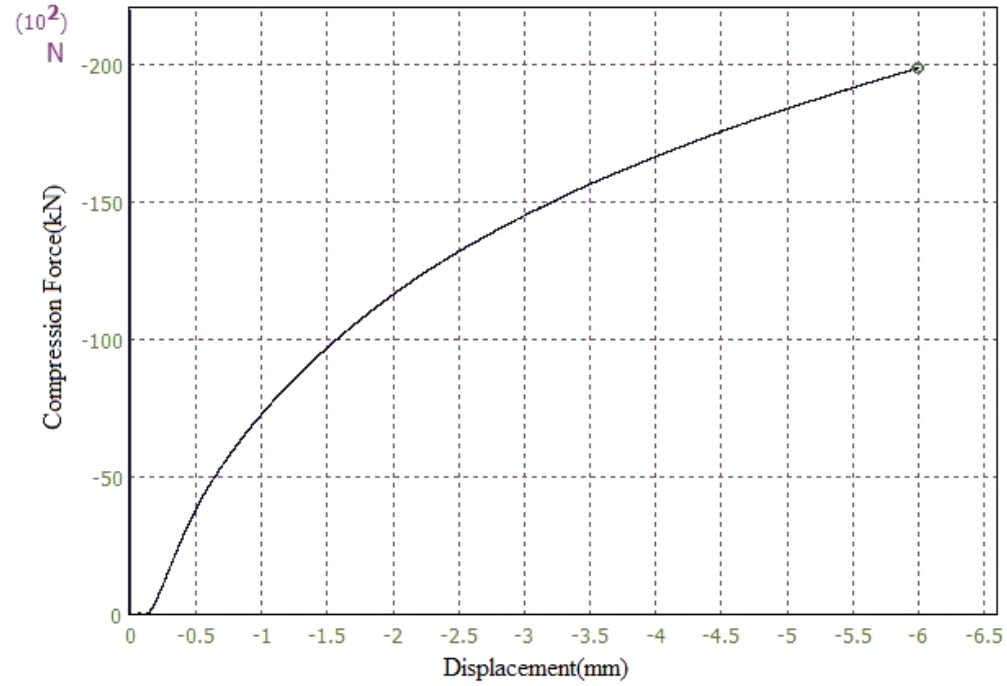

Figure 10. Compression force diagram for a 6 mm press stroke in a tube with an internal diameter of 18 mm

The diagram of changes in compressive force for 9 mm press stroke for tubes with inner diameters of 18 and 12 mm is shown in Figure 11. According to the diagram, as expected, the curve of the forming force of the tube with a smaller inner diameter is higher than the curve of the force of the tube with a larger diameter, and at the end of the press stroke, its force value is three times.

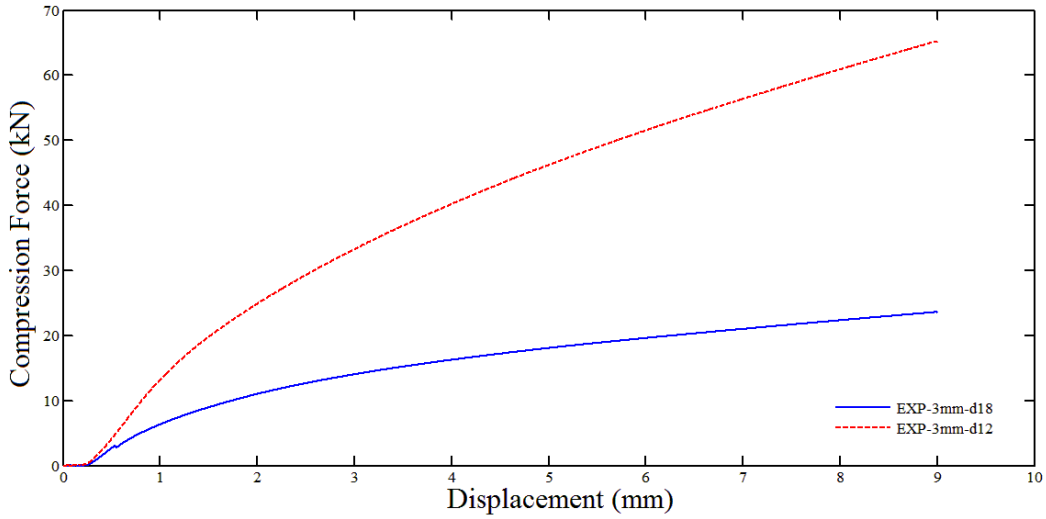

Figure 11. Comparison of the changes of compression force in terms of displacement for 9 mm press stroke in tubes of 18 and 12-mm inner diameters

2.4 Finite element simulation

ABAQUS software is used to simulate the process. The dies are modeled rigidly and properties such as density, modulus of elasticity, Poisson's ratio, and plastic properties have been entered into the software for aluminum tubes. The density of 2700 kg/m^3, Poisson's ratio of 0.33, and Young's modulus of 70 GPa are inputted in the software. The speed of the die movement was also 2 mm/min, similar to the speed of the simple tensile test. The lower die is fully tied until it is fixed in place and the upper die is moved vertically down by 3, 6, and 9 mm. In the tube with an inner diameter of 18 mm, the thickness of the tube is divided into three elements, and in the tube with an inner diameter of 12 mm, the thickness of the tube is divided into four elements. Figure 12 shows the templates and the meshed tube in the ABAQUS software.

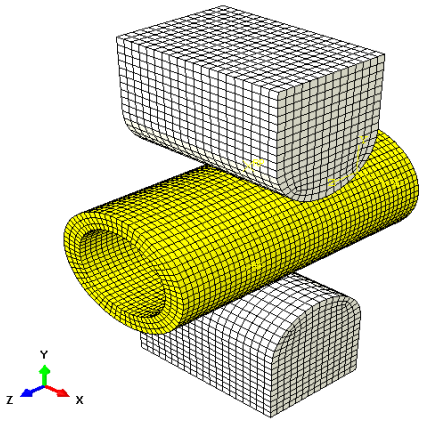

Figure 12. Dies and tubes in the ABAQUS software environment

Figure 13 shows the deformation created in the tubes. In both experimental and simulation methods, no noticeable increase in the length of the tube is observed.

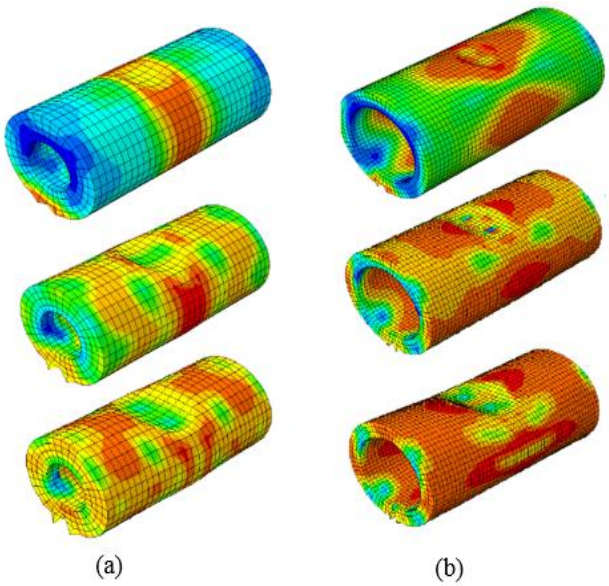

Figure 13. The deformed tubes a) Tube with an internal diameter of 18 mm in three press strokes of 3, 6, and 9 mm from top to bottom respectively b) Tube with an inner diameter of 12 mm in three press strokes of 3, 6, and 9 mm, respectively, from top to bottom

3. Results and discussion

3.1 Comparison of compression forces

In this section, applied forces obtained in simulation and experimental tests are compared. Figure 14 shows the curve of the changes of the compression force according to the press stroke for a 9 mm press stroke for a tube with an internal diameter of 18 mm. According to this diagram, the values of the forces differ by an average of 9%. Figure 16 shows the curve of the changes of the compression force according to the press stroke for a 9 mm press stroke for a tube with an inner diameter of 12 mm. In this example, the values of the forces differ by an average of 5%.

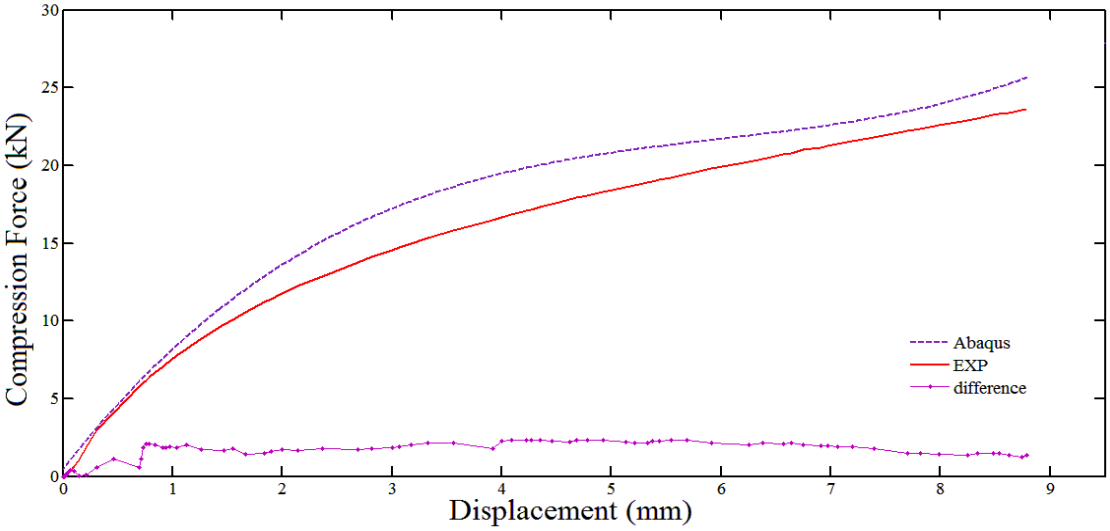

Figure 14. Comparison of force-displacement diagrams resulting from experimental method and simulation of 9 mm press stroke in a tube of 18 mm inner diameter

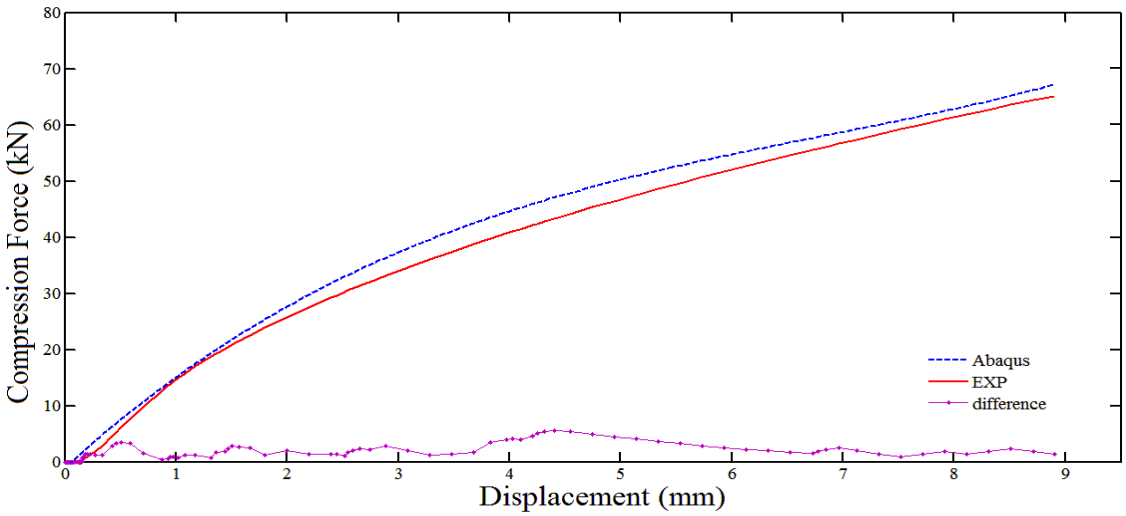

Figure 15. Comparison of force-displacement diagrams resulting from experimental method and simulation of 9 mm press stroke in a tube with an inner diameter of 12 mm

Comparison of Figures 11, 14, and 15 shows that the compression force curves obtained from the FE simulation are higher than the experimental force curves. This issue is due to the presence of small holes, impurities, etc. in the tube under test, which do not exist in the simulated tube.

3.2 Comparison of deformation zone

In this section, the deformations created in the tubes in different press strokes are measured and compared with the simulation results. To check the dimensions of Z and S parameters, according to Figure 16, it has been used. The parameter S represents the width of the tube, measured parallel to the axis of the die, in the deformation zone, and the parameter Z represents the amount of depression of the tube along the application of compressive force. Index c corresponds to the center of the tube and indices 1 to 5 are the values measured along the length of the tube. Since the values of S show the amount of lateral expansion of the tube due to the compressive force of the dies, the higher its value is than the initial diameter (25 mm), the greater the expansion, and the closer it is to the initial diameter, the less expansion. The projection of the contact surface between the die and the tube on the horizontal plane is almost oval, and the values E_1 and E_2 are its largest and smallest dimensions, respectively, in the transverse and longitudinal directions of the tube.

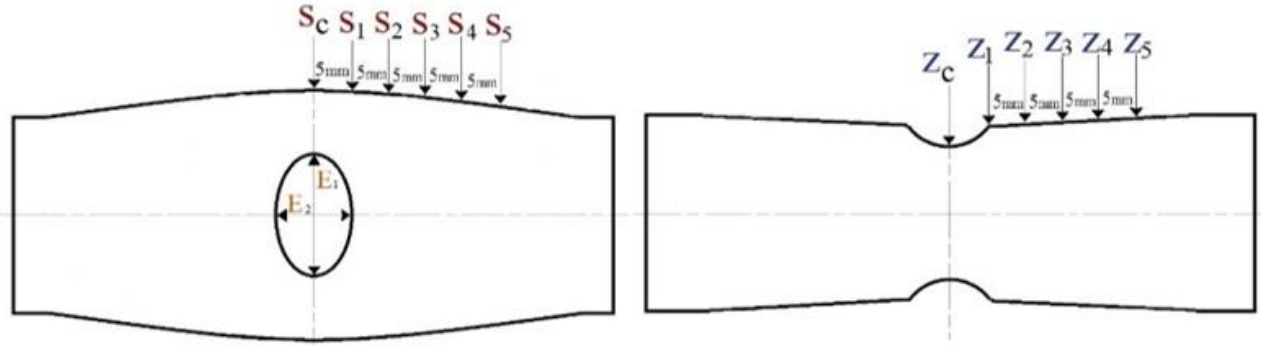

Figure 16. Dimensions measured on the deformed tube in two views

In Table 1, the deformation values of the tube for the 3 mm press stroke of the press machine obtained from experimental and simulation methods are shown in the sample with an internal diameter of 18 mm. A comparison of indentation values in two experimental and simulation methods shows that the values measured in the experimental method are lower than the simulation method. The difference in the dimensions is more in the center and gradually in the way of measuring the difference of the data, they tend to be zero. Comparing the expansion values for the two experimental and simulation methods shows that the expansion value of the tube in the experimental method is less than the simulation method, the biggest difference is seen in the S_1 diameter, and as the measurement is farther away from the center, the difference decreases. In all the tubes under investigation, the comparison of E_1 and E_2 values in the two experimental and simulation methods showed a very small difference, and therefore, they are not included in the tables. Also, the values of E_1 and E_2 in equal press strokes in the tube with an inner diameter of 12 mm are higher than the tube with an inner diameter of 18 mm, which indicates the greater resistance of the thicker tube and the smaller size of the deformation area.

Table 1. Comparison of 3mm press stroke deformation results from experimental and simulation methods for Tube sample with an internal diameter of 18 mm

	Z (mm)			S (mm)		
	Exp.	Sim.	Diff.	Exp.	Sim.	Diff.
C	22.92	22.01	0.91	25.50	25.73	0.23
1	24.32	23.49	0.80	25.40	25.66	0.26
2	24.82	24.3	0.43	25.30	25.4	0.10
3	24.92	24.6	0.32	25.12	25.31	0.19
4	25.00	24.7	0.22	25.08	25.10	0.02
5	25.00	25.00	0.00	25.00	25.07	0.07

A numerical comparison of tube deformation in a 3 mm press stroke obtained from experimental and simulation methods in a tube with an inner diameter of 12 mm is shown in Table 2. The recorded values of S in both experimental and simulation conditions show a very good agreement. Due to the difference in dimensions in this area, the amount of tube protrusion in the experimental method in S_c, S_2, S_3 coordinates is more than the corresponding values from the simulation method, and only in the size of S_1, the simulation value is more than the experimental method. The biggest difference is seen in S_c diameter and S_4 the difference has reached zero. The measured values of E_1 and E_2 in the experimental method show a smaller size than the simulation method. The difference between the dimensions in both methods is less than 1 mm, but it shows more values than the tube with an internal diameter of 18 mm with the same press stroke.

Table 2. Comparison of 3 mm press stroke deformation obtained from experimental and simulation methods in the tube with an inner diameter of 12 mm

	Exp. Z(mm)	Sim. Z(mm)	Diff. (mm)	Exp. S(mm)	Sim. S(mm)	Diff. (mm)
C	22.82	22.32	0.50	25.24	25.18	0.06
1	24.72	24.64	0.08	25.12	25.16	0.04
2	24.92	24.77	0.15	25.10	25.08	0.02
3	25.00	24.83	0.17	25.08	25.00	0.08
4	25.00	25.00	0.00	25.00	25.00	0.00
5	25.00	25.00	0.00	25.00	25.00	0.00

The comparison of the Z values in the 6 mm press stroke of the tube with an internal diameter of 18 mm, shown in Table 3, shows that the difference in the Z_c coordinates shows a large amount and according to the obtained dimensions, the indentation value in the simulation method is 1.12 mm is greater than the amount of indentation in the same coordinates of the experimental method.

Table 3. Comparison of deformation in 6 mm press stroke obtained from experimental and simulation methods in a tube with an inner diameter of 18 mm

	Exp. Z(mm)	Sim. Z(mm)	Diff.	Exp. S(mm)	Sim. S(mm)	Diff.
C	19.98	18.86	1.12	26.68	27.19	0.51
1	22.46	22.45	0.01	26.48	26.96	0.48
2	23.86	23.52	0.34	26.08	26.46	0.38
3	24.42	24.09	0.33	25.60	25.97	0.37
4	24.72	24.44	0.28	25.34	25.56	0.22
5	24.96	24.85	0.11	25.28	25.32	0.04

In Table 4, the numerical values of the amount of deformation in the press stroke of 6 mm obtained from the experimental and simulation methods in the tube with an inner diameter of 12 mm are given. The recorded values for Z in the press stroke of a 6 mm tube with an inner diameter of 12 mm show that the amount of indentation in the experimental method is slightly less than the simulation method in all points, that the greatest amount of data difference is in Z_c and in the following points the amount of difference is reduced and at the point Z_5 is zero. In general, a good match between the data is observed.

Table 4. Comparison of deformation in 6 mm press stroke obtained from experimental and simulation methods in a tube with an inner diameter of 12 mm

	Exp. Z(mm)	Sim. Z(mm)	Diff.	Exp. S(mm)	Sim. S(mm)	Diff.
C	20.00	18.91	0.82	25.82	25.87	0.05
1	23.84	23.08	0.70	25.70	25.76	0.06
2	24.60	24.33	0.27	25.32	25.42	0.10
3	24.88	24.61	0.27	25.20	25.10	0.10
4	24.96	24.78	0.18	25.08	25.00	0.08
5	25.00	25.00	0.00	25.00	25.00	0.00

The deformation dimensions of the press stroke for a 9 mm press stroke for a tube with an internal diameter of 18 mm are shown in Table 5. The recorded values of Z show a difference of 1.29 mm in Z_c and a difference of 1.13 mm in Z_1, and the difference has decreased in the following points. The reason for the large difference in the first two coordinates is the swelling or triangulation at the Z_c point and its effect on the Z_1 point in the simulation mode.

Also, according to the data, it can be seen that the amount of tube depression in the simulation method is more than in the experimental method. Due to the simulation conditions, it was not possible to measure Z_5. The S values show good agreement between experimental and simulation data. Also, the value of the protrusion recorded experimentally in the first 4 coordinates is higher than the value of the protrusion measured in the simulation.

Table 5. Comparison of the dimensions of the deformation area in the 9 mm press stroke obtained from the experimental and simulation methods in the tube with an internal diameter of 18 mm

	Exp. Z(mm)	Sim. Z(mm)	Diff. Z(mm)	Exp. S(mm)	Sim. S(mm)	Diff. S(mm)
C	17.26	15.97	1.29	28.26	28.10	0.16
1	21.00	19.87	1.13	28.04	27.78	0.26
2	22.56	21.93	0.63	27.12	27.06	0.06
3	23.84	23.08	0.76	26.50	26.30	0.20
4	24.30	23.74	0.56	25.88	25.70	0.18
5	24.72	--	--	25.40	25.52	0.12

The comparison of the dimensions of the deformation area for the 9 mm press stroke in the tube with an inner diameter of 12 mm is shown in Table 6. The numbers obtained for Z points in the experimental method show more values than the simulation method, which means that the indentation value calculated in the experimental method is lower than the simulation method. The largest data difference is in the Z_c coordinates, and in the following points, the difference between the obtained dimensions has decreased. The recorded values for S points show a good agreement between the dimensions obtained in both methods.

Table 6. Comparison of the deformation of the 9 mm press stroke resulting from the experimental and simulation method in the tube with an inner diameter of 12 mm

	Exp. Z(mm)	Sim. Z(mm)	Diff. Z(mm)	Exp.	Sim. S(mm)	Diff. S(mm)
C	17.32	16.27	0.96	26.76	26.91	0.15
1	23.32	22.45	0.87	26.42	26.67	0.25
2	24.22	23.99	0.23	25.78	25.92	0.14
3	24.72	24.51	0.21	25.32	25.43	0.11
4	24.88	24.75	0.13	25.18	25.10	0.08
5	24.98	--	--	25.10	25	0.10

4. Conclusions

- As expected, with the reduction of the inner diameter of the tube, and increasing the thickness of the tube, the required force to change the shape increases.
- By increasing the press stroke, the amount of compression force increases.

- In both experimental and simulation methods, no noticeable increase in the length of the tube was observed.
- The force value of the simulation method is higher than the experimental method.
- In the same press stroke, as the inner diameter of the tube increases, the size of the deformation area increases.
- The force difference between simulation and experimental data is greater in tubes with a smaller inner diameter.
- In the same press stroke, as the thickness of the tube increases, the size of the contact surface between the die and the tube decreases.

5. References

[1] Kobayashi, H. and Daimaruya, M. 1994. Dynamic and quasi-static lateral compression tests of ceramics tubes. Journal de Physique IV-Proceedings. 04:275-280. doi:10.1051/jp4:1994841.

[2] Avalle, M. and Goglio, L. 1999. Lateral compression of thin-walled tubes strain measurement by image analysis. Experimental Mechanics. 3:231-235. doi: 10. 1007/BF02323557.

[3] Gupta, N.K., Sekhon, G.S. and Gupta, P.K. 2005. Study of lateral compression of round metallic tubes. Thin-Walled Structures. 43:895–922. doi:10.1016/j.tws.2004.12.002.

[4] Niknejad, A., Ali Elahi, S. and Liaghat, Gh. H. 2011. Experimental investigation on the lateral compression in the foam-filled circular tubes. Materials and Design. 36:24-34. doi:10.1016/j.matdes.2011.10.047.

[5] Rathnaweera, G., Durandet, Y., Ruan D. and Kinoshita, S. 2011. Characterizing the material properties of a tube from a lateral compression test. International Journal of Protective Structures. 2:465-475. doi:10.1260/2041-4196.2.4.465.

[6] Schiemann, T., Liewald, M., Beiermeister, C. and Till, M. 2014. Influence of process chain on fold formation during flange upsetting of tubular cold forged parts. Procedia Engineering. 81:352 – 357. doi:10.1016/j.proeng.2014.10.005.

[7] Nomura, T., Nguyen, C.S., Asai, K. and Kitamura, K. 2016. Behavior of asymmetric deformation of rod in locally-lateral upsetting Mechanical Engineering Journal. 3:1-7. doi:10.1299/mej.15-00576.

[8] Parvizi Bina E. and Haghighat H. 2021. Limit analysis of plane strain compression of cylindrical billets between flat dies. Journal of Advanced Manufacturing Technology. 116:1-10. doi:10.1007/s00170-021-07711-1.

[9] Pepelnjak, T., Šašek, P. and Kudlaček J. 2016. Upsetting Analysis of High-Strength Tubular Specimens with the Taguchi Method. Metals. 6:257. doi:10.3390/met6110257.

[10] Guan, Y., Li, C, Guo, S. and Lin, P. 2022. A novel combined process of flaring-upsetting for forming end flanges on thin-walled tubes. Journal of Manufacturing Processes. 84:927-936. doi:10.1016/j.jmapro.2022.10.051.

[11] Zhang, Z. 2022. Theoretical prediction of cross-sectional deformation of circular thin-walled tube in large elastic–plastic deformation stage under lateral compression. Thin-Walled Structures. 180:109957. doi:10.1016/j.tws.2022.109957.